On the accuracy of finite element approximations of elliptic problems with heterogeneous coefficients

Giovanni Taraschi[1], Alisson S. Pinto[2], Cristiane O. Faria[2], Maicon R. Correa[1]

[1]*Departamento de Matemática Aplicada, IMECC, Unicamp*
Rua Sérgio Buarque de Holanda, 651, 13083-859, Campinas/SP, Brasil
gitaraschi@gmail.com, maicon@ime.unicamp.br
[2]*Instituto de Matemática e Estatística, UERJ*
Rua São Francisco Xavier, 524, 6º andar, 20550-900, Rio de Janeiro/RJ, Brasil
alisson.pinto@pos.ime.uerj.br, cofaria@ime.uerj.br

Abstract. In this work, we investigate the accuracy of different finite element post-processing strategies in the approximation of dual fields in elliptic problems such the stress tensor field in the linear elasticity problem, with special attention to problems with discontinuous coefficients.

Keywords: Finite element methods, Post-processings, Heterogeneous coefficients, Interface of discontinuity

1 Introduction

The development of accurate and stable finite element methods for elliptic problems is related to the choice of the main unknowns variables and the respective finite-dimensional subspaces for their approximation. Some classical examples of unknowns/problems are the displacement and the stress tensor in the linear elasticity and the flux and the pressure in the Darcy problem. For instance, let Ω be a bounded open subset in $\mathbb{R}^2$, with a Lipschitz continuous boundary $\partial\Omega$. If Ω represents the domain of a rigid porous medium saturated with an incompressible fluid, the relation between the gradient of the poro-pressure $p : \Omega \to \mathbb{R}$ and the averaged (Darcy's) velocity $\boldsymbol{v} : \Omega \to \mathbb{R}^2$ is given by the well-known Darcy's law (Correa et al. [1])

$$\boldsymbol{v} = -\mathcal{K}\,\nabla p \quad \text{in } \Omega, \tag{1}$$

where $\mathcal{K} = \mathcal{K}(\boldsymbol{x})$ is a symmetric and uniformly positive definite tensor representing the permeability of the porous matrix divided by the fluid viscosity. The Darcy problem is determined by including the mass balance equation

$$\operatorname{div} \boldsymbol{v} = f \quad \text{in } \Omega, \tag{2}$$

and appropriate boundary conditions, where f is a distributed source/sink function. Similarly, if Ω represents a domain occupied by a linear elastic body, the deformation suffered is related to the stress field $\boldsymbol{\sigma} : \Omega \to \mathbb{S}$, where $\mathbb{S} = \mathbb{R}^{2\times 2}_{\text{sym}}$ is the space of symmetric second order real tensors, through the constitutive equation (Arnold [2], Quinelato et al. [3])

$$\boldsymbol{A}\boldsymbol{\sigma} = \boldsymbol{\varepsilon}(\boldsymbol{u}) \quad \text{in } \Omega. \tag{3}$$

$\boldsymbol{u} : \Omega \to \mathbb{R}^2$ is the displacement field, $\boldsymbol{\varepsilon}(\boldsymbol{u})$ is the corresponding infinitesimal strain tensor, given by the symmetric part of the gradient of $\boldsymbol{u}$,

$$\boldsymbol{\varepsilon}\left(\boldsymbol{u}\right) = \nabla^s \boldsymbol{u} = \frac{1}{2}\left(\nabla \boldsymbol{u} + \left(\nabla \boldsymbol{u}\right)^t\right).$$

The material properties are determined by the compliance tensor $\boldsymbol{A}$, which is a positive definite symmetric operator from $\mathbb{S}$ to itself, possibly depending on the point $\boldsymbol{x} \in \Omega$ (Arnold [2]). In the isotropic case it is

$$\boldsymbol{A}\boldsymbol{\sigma} = \frac{1}{2\mu}\left(\boldsymbol{\sigma} - \frac{\lambda}{2\left(\lambda+\mu\right)}\operatorname{tr}\left(\boldsymbol{\sigma}\right)\boldsymbol{I}\right), \tag{4}$$

where $\lambda \geq 0$ and $\mu > 0$ are the Lamé coefficients and $\boldsymbol{I}$ denotes the identity tensor. The inverse of $\boldsymbol{A}$ is the elasticity tensor $\boldsymbol{C} : \mathbb{S} \to \mathbb{S}$, that in the isotropic case is given by

$$\boldsymbol{C}\boldsymbol{\varepsilon} = 2\mu\boldsymbol{\varepsilon} + \lambda \operatorname{tr}(\boldsymbol{\varepsilon})\boldsymbol{I} = \boldsymbol{\sigma}. \tag{5}$$

The system of the linear elasticity problem are closed by the introduction of the equilibrium equation, which states the conservation of linear momentum,

$$\operatorname{div} \boldsymbol{\sigma} = \boldsymbol{g} \quad \text{in } \Omega, \tag{6}$$

and $\boldsymbol{g}$ denotes the imposed volume load. The divergence operator div applies to the matrix field $\boldsymbol{\sigma}$ row-by-row.

The systems eq. (1)-(2) (Darcy problem) and eq. (3)-(6) (Elasticity problem) are prototypes of elliptic problems (Arnold [2]), written as systems of first-order PDEs. Using the finite element terminology, there are two main approaches to solve such systems: the use of *Mixed methods* (Quinelato et al. [3], Raviart and Thomas [4], Arbogast and Correa [5]), that are based on the simultaneous approximation of the pairs $(p, \boldsymbol{v})$ and $(\boldsymbol{u}, \boldsymbol{\sigma})$, and the use of *Primal methods* (Arnold [2], Raviart and Thomas [6]), that are based on the second order elliptic PDE for the primal variable (poro-pressure for Darcy and displacement for Elasticity), which is obtained by replacing the constitutive equation in the balance equation. The main characteristic of the Mixed methods is the use of different finite element spaces for each variable. In order to provide stable numerical solutions, the spaces need to be compatible in the sense that they must satisfy conditions such as the ellipticity on the kernel and the inf-sup condition (Arnold [2]). This compatibility requirement reduces the flexibility in constructing such subspaces, implying on a higher code complexity, when compared to the Primal methods (Correa et al. [1]). Within the Primal methods, the primal field can be approximated by using different Finite Element strategies, such as the classical H^1-conforming Galerkin (Arnold [2]), Primal-Hybrid Formulations (Raviart and Thomas [6]), and Discontinuous Galerkin Methods (Arnold et al. [7]). The approximation of the primal field using the classical H^1-conforming Galerkin method (Arnold [2]) leads to optimal-order solutions, but the evaluation of the dual field demands a post-processing strategy. The post-processing can be local, such as taking the gradient of the solution for the primal variable and using the constitutive equation, or can be evaluated by setting a new problem in patches of elements or in the whole domain (Loula et al. [8], Correa and Loula [9]). The aim of post-processing techniques is to provide approximations for the dual variable with continuous normal components between adjacent elements and good mass conservation properties (Correa et al. [1]).

In Loula et al. [8] the authors presented a family of higher-order gradient post-processings for second order elliptic problems, including global, element-by-element and macroelement strategies based on least-squares residuals of the balance law and the constitutive equation. Although other primal methods can be employed, the proposed post-processings used the gradient of the primal solution obtained by the H^1-conforming Galerkin method as a source for the evaluation of the dual variable. Both classical Lagrangian H^1-conforming (nodal continuous) finite element spaces and $H(\operatorname{div})$-conforming finite element subspaces (such as the Raviart-Thomas spaces in Raviart and Thomas [4]) can be used for the approximation of the Darcy velocity and the stresses. In particular, the continuous Lagrangian strategy can be easily implemented as standard single field formulations, with great flexibility in the choice of the finite element spaces (Loula et al. [8]). However, the results presented in Correa and Loula [9] and Loula et al. [10] for the Darcy problem with discontinuous permeability fields, showed that the Darcy velocity approximated by continuous Lagrangian elements is subject to spurious oscillations due to the imposition of continuity on the tangent components of the velocity field on the interface of the elements.

In the present work we follow the steps of Correa and Loula [9] and show that a similar drawback happens when the continuous Lagrangian global post-processing of Loula et al. [8] is used to approximate the stress field in problems where the Lamé coefficients are discontinuous. In this case the spurious results are due to the imposition of nodal continuity to the vector $\boldsymbol{\sigma\tau}$, where $\boldsymbol{\tau}$ is the unitary vector tangent to the interface of discontinuity. In order to do so, first we present in Section 2 the global post-processing of Loula et al. [8], in the context of the linear Elasticity problem, and also an alternative local stress-recovery strategy that guarantees the continuity of the traction vector $\boldsymbol{\sigma n}$, where $\boldsymbol{n}$ is the unitary outward vector, normal to the element edges. Then, in Section 3 we perform convergence studies in two different problems. The first one has homogeneous Lamé coefficients and is intended to confirm the a-priori estimates established in Loula et al. [8] for the use of the continuous Lagrangian global post-processing to problems with smooth solutions. The second one has an interface of discontinuity of the Lamé coefficients and is specially constructed to have a solution with continuous traction vector $\boldsymbol{\sigma n}$ but discontinuous vector $\boldsymbol{\sigma\tau}$. Finally, conclusions are given in Section 4.

2 Finite element post-processings

Let $L^2(T, Y)$ be the space of square integrable functions with domain $T \subset \mathbb{R}^2$, taking values in the finite-dimensional vector space Y, with inner product $(\cdot, \cdot)$ and norm $\| \cdot \|_0 = \| \cdot \|$. We denote by $H^m(T, Y)$ the

Sobolev space consisting of functions with all derivatives of order at most m square integrable, with norm $\|\cdot\|_m$ and seminorm $|\cdot|_m$ and the space $H(\mathrm{div}, T, Y)$ of square-integrable fields with square-integrable divergence, as usual. We similarly denote by $\mathbb{P}_k(T, Y)$ the space of polynomial functions on T of degree at most k taking values in Y, and by $\mathbb{P}_{k_1,k_2}(T, Y)$ the space of polynomial functions on T of degree at most $k_1 \geq 0$ in $x = x_1$ and degree at most $k_2 \geq 0$ in $y = x_2$, taking values in Y. The range space Y will be either $\mathbb{R}$, $\mathbb{R}^2$, $\mathbb{S}$ or $\mathbb{M} = \mathbb{R}^{2\times 2}$.

2.1 Primal formulation

The elliptic problem posed on displacement field only is found by replacing the strain-stress relation eq.(5) in the equilibrium equation, eq. (6), given

$$\mathrm{div}\,(\boldsymbol{C}\boldsymbol{\varepsilon}(\boldsymbol{u})) = \boldsymbol{g} \quad \text{in } \Omega, \qquad \boldsymbol{u} = \boldsymbol{0} \quad \text{on } \partial\Omega, \tag{7}$$

that is the basis for the definition of the standard primal Galerkin method (Arnold [2]). For simplicity we only consider homogeneous Dirichlet boundary conditions, although other boundary conditions could be handled in the usual ways. It is important to remark that this standard method is suitable for compressible problems. For incompressible problems, when the Poisson ratio $\nu = \lambda/2(\lambda + \mu)$ approaches to $1/2$ (i.e., $\lambda \to \infty$), the elasticity tensor $\boldsymbol{C}$ becomes infinite, and a mixed formulation must be employed as Arnold [2] and Quinelato et al. [3]. The classical primal variational formulation of eq. (7) consists on finding the displacement field $\boldsymbol{u} \in \mathcal{U}$ such that

$$\int_\Omega \boldsymbol{C}\boldsymbol{\epsilon}(\boldsymbol{u}) : \boldsymbol{\epsilon}(\boldsymbol{v})\,\mathrm{dx} = -\int_\Omega \boldsymbol{g}\cdot\boldsymbol{v}\,\mathrm{dx}, \quad \forall\, \boldsymbol{v} \in \mathcal{U}, \tag{8}$$

with $\mathcal{U} = \left\{\boldsymbol{v} \in H^1(\Omega, \mathbb{R}^2); \boldsymbol{v} = \boldsymbol{0} \text{ on } \partial\Omega\right\}$. Let $\{\mathcal{T}_h\}$ be a family of partitions $\mathcal{T}_h = \{K\}$ of Ω, indexed by the parameter h, which represents the maximum diameter of the elements $K \in \mathcal{T}_h$. Henceforth we assume that the elements K are convex quadrilaterals, but the results also hold for triangular elements. Denoting by $\hat{K}$ the standard reference element, in our case the unit square $[0, 1] \times [0, 1]$, each geometrical element $K \in \mathcal{T}_h$, is generated from an isomorphism $F_K : \hat{K} \to \mathbb{R}^2$ such that $K = F_K(\hat{K})$. Assume that we take finite-dimensional subspace $\mathcal{U}_h^k \subset \mathcal{U}$ composed of continuous piecewise Lagrangian polynomials of degree $k \geq 1$, given by

$$\mathcal{U}_h^k = \left\{\boldsymbol{v}_h \in \mathcal{U};\ \boldsymbol{v}_h|_K \in F_K(\mathbb{P}_{k,k}(\hat{K}, \mathbb{R}^2))\,\forall K \in \mathcal{T}_h\right\}, \tag{9}$$

then it is well known that the Galerkin method to eq. (8) yields to convergent approximate solutions $\boldsymbol{u}_h \in \mathcal{U}_h^k$ (Arnold [2]). The Galerkin local post-processing for the stress can then be defined by taking the gradient of the solution $\boldsymbol{u}_h$ element by element and using the constitutive equation, eq. (5),

$$\boldsymbol{\sigma}_h^{\mathrm{G}}\big|_K = \boldsymbol{C}\boldsymbol{\epsilon}(\boldsymbol{u}_h)\big|_K \quad \forall K \in \mathcal{T}_h. \tag{10}$$

In this case, for regular solutions, Arnold [2] holds the following estimates

$$\|\boldsymbol{u} - \boldsymbol{u}_h\| \leq Ch^{k+1}|\boldsymbol{u}|_{k+1} \quad \text{and} \quad \|\boldsymbol{\sigma} - \boldsymbol{\sigma}_h^{\mathrm{G}}\| \leq Ch^k|\boldsymbol{u}|_{k+1}. \tag{11}$$

Although convergent, this strategy leads to locally discontinuous stresses, do not fulfilling the requirement of continuous traction vectors.

2.2 Global post-processing

Now, let $\mathcal{S}_h$ be a finite element subspace of $H(\mathrm{div}, \Omega, \mathbb{S})$ and $\boldsymbol{u}_h \in \mathcal{U}_h^k$ the previously defined Galerkin solution of eq. (7). The global post-processing of Loula et al. [8] combines the least-squares residuals of eq. (3) and eq. (6) and defines the approximate stress field $\boldsymbol{\sigma}_h^{\mathrm{P}} \subset \mathcal{S}_h$ as the solution of the finite-dimensional variational problem

$$\int_\Omega \boldsymbol{A}\boldsymbol{\sigma}_h^{\mathrm{P}} : \boldsymbol{\tau}_h\,\mathrm{dx} + (\delta h)^\alpha \int_\Omega \mathrm{div}\,\boldsymbol{\sigma}_h^{\mathrm{P}}\cdot\mathrm{div}\,\boldsymbol{\tau}_h\,\mathrm{dx} = \int_\Omega \boldsymbol{\varepsilon}(\boldsymbol{u}_h) : \boldsymbol{\tau}_h\,\mathrm{dx} + (\delta h)^\alpha \int_\Omega \boldsymbol{g}\cdot\mathrm{div}\,\boldsymbol{\tau}_h\,\mathrm{dx}, \quad \forall \boldsymbol{\tau}_h \in \mathcal{S}_h, \tag{12}$$

with δ and α positive real parameters. The analysis presented in Loula et al. [8] covers the use of both continuous Lagrangian and $H(\mathrm{div})$-conforming constructions of $\mathcal{S}_h$. In particular, the use of the continuous Lagrangian based subspace of degree l, given by

$$\mathcal{S}_h^l = \left\{\boldsymbol{\tau}_h \in H^1(\Omega, \mathbb{S});\ \boldsymbol{\tau}_h|_K \in F_K(\mathbb{P}_{k,k}(\hat{K}, \mathbb{S}))\,\forall K \in \mathcal{T}_h\right\}, \tag{13}$$

leads to the following a-priori error estimate for the stress

$$\|\boldsymbol{\sigma} - \boldsymbol{\sigma}_h^{\mathrm{P}}\|_0 \leq C(h^{l+\alpha/2}|\boldsymbol{\sigma}|_{l+1} + h^{k+1-\alpha/2}|\boldsymbol{u}|_{k+1}). \tag{14}$$

Notice that the approximate solution $\boldsymbol{\sigma}_h^{\mathrm{P}}$ is fully continuous. Thus, as explained in the introduction, we can expect difficulties in the approximation of problems where the solution presents an interface of discontinuity.

2.3 Local stress recovery

The local stress recovery strategy makes use of an approximation $\boldsymbol{t}_h$ for the traction vector $\boldsymbol{t} = \boldsymbol{\sigma}\boldsymbol{n}$, uniquely defined on the edges of the partition $\mathcal{T}_{\mathrm{h}}$. From $\boldsymbol{t}_h$ we construct an unique stress approximation $\boldsymbol{\sigma}_h^{\mathrm{L}} \in \mathcal{RT}_0(\Omega, \mathbb{R}^2) \times \mathcal{RT}_0(\Omega, \mathbb{R}^2)$ such that, for each element $K \in \mathcal{T}_{\mathrm{h}}$, the following local systems are satisfied

$$\int_{\partial K} \boldsymbol{\sigma}_h^{\mathrm{L}} \boldsymbol{n} \cdot \boldsymbol{e}_i \, \mathrm{ds} = \int_{\partial K} \boldsymbol{t}_h \cdot \boldsymbol{e}_i \, \mathrm{ds}, \quad i = 1 \text{ and } 2, \tag{15}$$

where $\boldsymbol{e}_i$ denotes the i-th canonical vector of $\mathbb{R}^2$. $\mathcal{RT}_0(\Omega, \mathbb{R}^2)$ is the lowest order Raviart-Thomas space, which in quadrilateral meshes is given by

$$\mathcal{RT}_0(\Omega, \mathbb{R}^2) = \{\boldsymbol{v} \in H(\mathrm{div}, \Omega, \mathbb{M});\ \boldsymbol{v}|_K \in \mathcal{P}_{F_K}(\mathbb{P}_{1,0}(\hat{K}, \mathbb{R}^2) \times \mathbb{P}_{0,1}(\hat{K}, \mathbb{R}^2)),\ \forall K \in \mathcal{T}_{\mathrm{h}}\}, \tag{16}$$

where $\mathcal{P}_{F_K}$ denotes the Piola's transform between $\hat{K}$ and K. Since $\boldsymbol{t}_h$ is uniquely determined, eq. (15) guarantees that $\boldsymbol{\sigma}_h^L$ has continuous traction. In this work, we take for the internal edges

$$\boldsymbol{t}_h|_e = \frac{1}{2}\left(\boldsymbol{C}|_{K_1}\, \boldsymbol{\varepsilon}(\boldsymbol{u}_h|_{K_1}) + \boldsymbol{C}|_{K_2}\, \boldsymbol{\varepsilon}(\boldsymbol{u}_h|_{K_2})\right)\boldsymbol{n}, \tag{17}$$

where $\boldsymbol{n}$ is the unitary vector normal to e and K_1 and K_2 are the two elements sharing the edge e. If the edge e is on the boundary $\partial\Omega$, we simply take $\boldsymbol{t}_h|_e = \boldsymbol{C}\boldsymbol{\varepsilon}(\boldsymbol{u}_h)\boldsymbol{n}$.

3 Numerical experiments

In this section we perform a set of numerical experiments to evaluate the behaviour of the post-processing techniques discussed in Section 2. The numerical experiments are divided into two parts. In the first one we propose and solve an isotropic and homogeneous problem with the exact solutions $\boldsymbol{u}$ and $\boldsymbol{\sigma}$ being continuous in the whole domain. In the second part we propose an heterogeneous problem, defined on the same domain and with the same exact solution for the displacement as the previous problem, but now the stress tensor $\boldsymbol{\sigma}$ has a tangential interface discontinuity. In both problems the domain $\Omega = [-1, 1] \times [-1, 1]$ is divided into $n \times n$ square elements, with $n = 8, 16, 32, 64$ and 128. The exact solution for the displacement is

$$\boldsymbol{u}(x, y) = \begin{bmatrix} -\frac{\pi}{2} y^2 \cos(\pi x) - 10xy \\ y \sin(\pi x) + 5x^2 \end{bmatrix}, \tag{18}$$

and numerical solution $\boldsymbol{u}_h$ is obtained by the Galerkin method with the space $\mathcal{U}_h^1$. Dirichlet boundary conditions are imposed on the sides $y = -1$ and $y = 1$ and Neumann conditions are imposed on the sides $x = -1$ and $x = 1$. Approximations for the stress field are then computed by three different post-processing strategies. In the global post-processing, the stresses were approximated in the space $\mathcal{S}_h^1$ and the symmetry of $\boldsymbol{\sigma}$ was strongly enforced by imposing that $\boldsymbol{\sigma}_{1,2} = \boldsymbol{\sigma}_{2,1}$. We also set $\delta = 1$ and $\alpha = 1$ since, according to the analysis developed in Loula et al. [8], this choice leads to improved convergence rates for $\boldsymbol{\sigma}_h$. Finally, the third strategy approximates $\boldsymbol{\sigma}$ by the stress recovery strategy described in Section 2.3, using the lowest order Raviart-Thomas space $\mathcal{RT}_0$. We notice that in this strategy, the symmetry of $\boldsymbol{\sigma}$ is not imposed, but the continuity of the traction vector is satisfied.

Homogeneous test problem For the first set of experiments we solve the model problem (7) by setting

$$\boldsymbol{g}(x, y) = \begin{bmatrix} (\frac{9\pi^3}{2} y^2 + \pi)\cos(\pi x) \\ \frac{\pi^2}{10} y \sin(\pi x) - 1 \end{bmatrix} \quad \text{and} \quad \boldsymbol{C}\boldsymbol{\varepsilon}(\boldsymbol{u}) = 0.8\boldsymbol{\varepsilon}(\boldsymbol{u}) + 0.1\,\mathrm{div}(\boldsymbol{u})\boldsymbol{I}.$$

The exact solution for the stress tensor can be easily obtained from eq. (18) and eq. (3), which we notice that it has continuous components in the whole domain. Table 1 presents the L^2 errors and the convergence rates for the

approximation of $\boldsymbol{u}$ by the Galerkin method, and the approximation of $\boldsymbol{\sigma}$ by post-processing strategies. The results are in agreement with the error estimate eq. (11) for $k = 1$ and are slight better than the predicted for the global post-processing given by eq. (14), with $k = l = \delta = \alpha = 1$. A comparison between the approximated solutions for the $\sigma_{1,1}$, $\sigma_{1,2}$ and $\sigma_{2,2}$ components of the the stress field obtained by the different post-processing strategies is presented in Figures 1, 2 and 3, respectively.

Table 1. L^2 errors and its convergence rates in the approximation of $\boldsymbol{u}$ and $\boldsymbol{\sigma}$ using the three post-processing approaches for the homogeneous problem.

	$\|\boldsymbol{u} - \boldsymbol{u}_h\|_{0,\Omega}$		$\|\boldsymbol{\sigma} - \boldsymbol{\sigma}_h^{\mathrm{G}}\|_{0,\Omega}$		$\|\boldsymbol{\sigma} - \boldsymbol{\sigma}_h^{\mathrm{L}}\|_{0,\Omega}$		$\|\boldsymbol{\sigma} - \boldsymbol{\sigma}_h^{\mathrm{P}}\|_{0,\Omega}$	
n	err.	rate	err.	rate	err.	rate	err.	rate
8	1.3596e-01	1.97	1.1001e+00	0.99	1.5673e+00	1.05	4.6879e-01	1.26
16	3.4263e-02	1.99	5.5141e-01	1.00	7.5189e-01	1.06	1.1452e-01	2.03
32	8.5843e-03	2.00	2.7589e-01	1.00	3.6772e-01	1.03	2.4455e-02	2.23
64	2.1472e-03	2.00	1.3797e-01	1.00	1.8198e-01	1.01	5.5793e-03	2.13
128	5.3688e-04	2.00	6.8987e-02	1.00	9.0551e-02	1.01	1.3730e-03	2.02

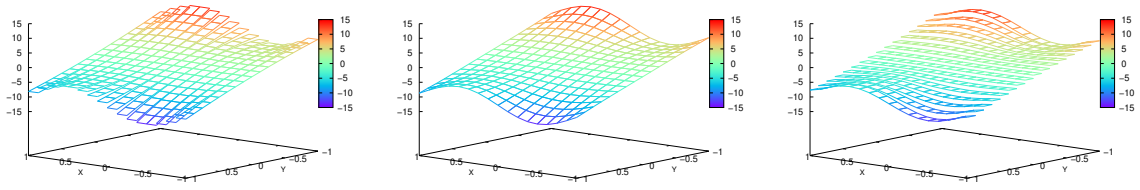

Figure 1. Homogeneous problem: component $\sigma_{1,1}$ of the stress field approximated with the local Galerkin, the global post-processing and the local stress recovery strategy.

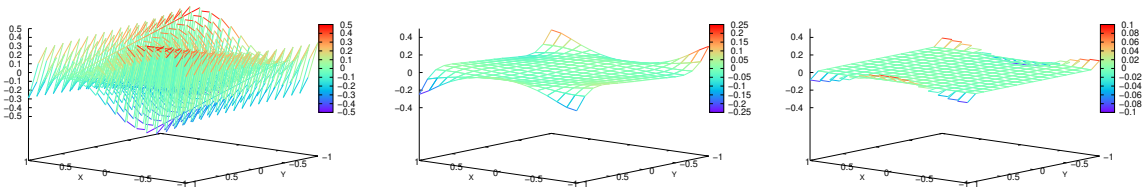

Figure 2. Homogeneous problem: component $\sigma_{1,2}$ of the stress field approximated with the local Galerkin, the global post-processing and the local stress recovery strategy.

Heterogeneous test problem In this second experiment we set the source term as

$$\boldsymbol{g}(x,y) = \begin{bmatrix} (\frac{9\pi^3}{2}y^2 + \pi)\cos(\pi x) \\ \frac{\pi^2}{10}y\sin(\pi x) - 1. \end{bmatrix} \text{ if } x \geq 0 \text{ and } \boldsymbol{g}(x,y) = \begin{bmatrix} (\frac{9\pi^3}{2}y^2 + \pi)\cos(\pi x) \\ \frac{7\pi^2}{10}y\sin(\pi x) - 7. \end{bmatrix}, \text{ otherwise.}$$

For the elasticity tensor $\boldsymbol{C}$ we adopt

$$\boldsymbol{C}\boldsymbol{\varepsilon}(\boldsymbol{u}) = 0.8\boldsymbol{\varepsilon}(\boldsymbol{u}) + 0.1\,\mathrm{div}(\boldsymbol{u})\boldsymbol{I} \text{ if } x \geq 0 \text{ and } \boldsymbol{C}\boldsymbol{\varepsilon}(\boldsymbol{u}) = 0.2\boldsymbol{\varepsilon}(\boldsymbol{u}) + 0.7\,\mathrm{div}(\boldsymbol{u})\boldsymbol{I}, \text{ otherwise.}$$

In addition to the introduction of an heterogeneity on the elasticity tensor, another major difference between the first and the second test problem relies on the exact solution for $\boldsymbol{\sigma}$, which now presents a discontinuity in the component $\sigma_{2,2}$ on the interface $x = 0$. The results presented in Table 2 show that the convergence rates of the

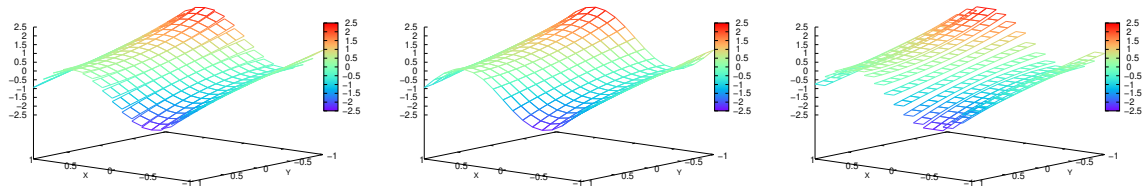

Figure 3. Homogeneous problem: component $\sigma_{2,2}$ of the stress field approximated with the local Galerkin, the global post-processing and the local stress recovery strategy.

stress $\boldsymbol{\sigma}_h^{\mathrm{P}}$ approximated by the Lagrangian global post-processing, drops to $\mathcal{O}(h^{0.5})$. As expected, this bad result is a consequence of the imposition of nodal continuity for the approximate stress on the interface, as can be seen on the results shown in Figures 4, 5 and 6. It is important to note that, among the three post-processings, the local stress recovery was the only strategy capable of accurately represent the continuity of the component $\sigma_{1,1}$ and the discontinuity of the component $\sigma_{2,2}$.

Table 2. L^2 errors and convergence rates in the approximation of $\boldsymbol{u}$ and $\boldsymbol{\sigma}$ using the three post-processing approaches for the heterogeneous problem.

	$\|\boldsymbol{u}-\boldsymbol{u}_h\|_{0,\Omega}$		$\|\boldsymbol{\sigma}-\boldsymbol{\sigma}_h^{\mathrm{G}}\|_{0,\Omega}$		$\|\boldsymbol{\sigma}-\boldsymbol{\sigma}_h^{\mathrm{L}}\|_{0,\Omega}$		$\|\boldsymbol{\sigma}-\boldsymbol{\sigma}_h^{\mathrm{P}}\|_{0,\Omega}$	
n	err.		err.	rate	err.	rate	err.	rate
8	1.5206e-01	1.86	9.6093e-01	0.97	1.6151e+00	1.03	1.0970e+00	0.75
16	4.0360e-02	1.91	4.8665e-01	0.98	7.8272e-01	1.05	7.2001e-01	0.61
32	1.0316e-02	1.97	2.4448e-01	0.99	3.8455e-01	1.03	5.0402e-01	0.51
64	2.5965e-03	1.99	1.2241e-01	1.00	1.9068e-01	1.01	3.5651e-01	0.50
128	6.5046e-04	2.00	6.1227e-02	1.00	9.4965e-02	1.01	2.5241e-01	0.50

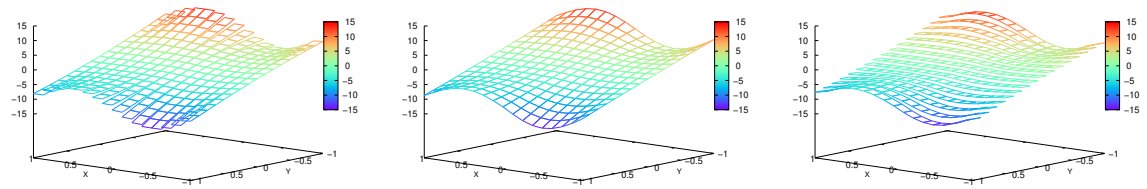

Figure 4. Heterogeneous problem: component $\sigma_{1,1}$ of the stress field approximated with the local Galerkin, the global post-processing and the local stress recovery strategy.

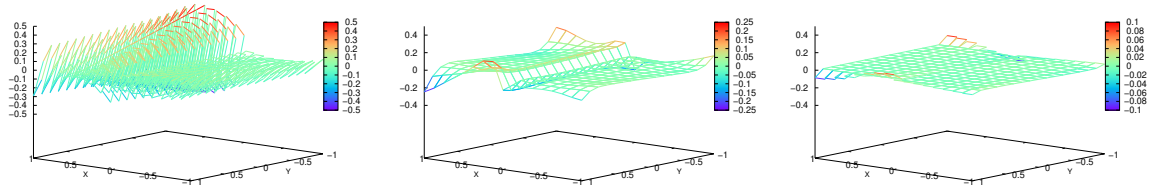

Figure 5. Heterogeneous problem: component $\sigma_{1,2}$ of the stress field approximated with the local Galerkin, the global post-processing and the local stress recovery strategy.

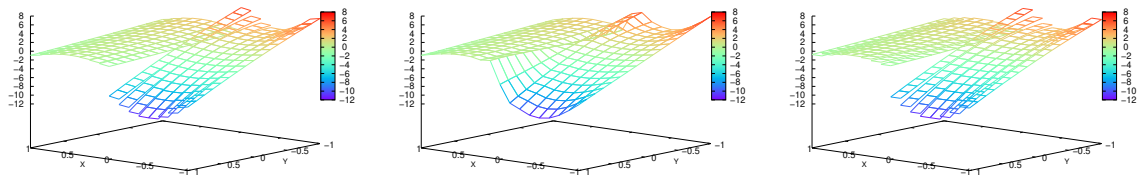

Figure 6. Heterogeneous problem: component $\sigma_{2,2}$ of the stress field approximated with the local Galerkin, the global post-processing and the local stress recovery strategy.

4 Conclusions

In this work, we studied the accuracy and the convergence behavior of three post-processing strategies for the approximation of the dual variable in an elliptic problem with discontinuous coefficients, namely the stress field in the linear elasticity problem. The results confirm the predictions that the global post-processing strategy with continuous Lagrangian approximations for the stress is not appropriate for the solution of problems with discontinuous coefficients. A simple local stress recovery strategy, based on the lowest index Raviart-Thomas elements, was the only one capable of accurately represent the continuity/discontinuity constraints of the stress field in the heterogeneous test.

Acknowledgements. The authors thankfully acknowledge the financial support from the research agencies. This work was funded by the National Council for Scientific and Technological Development - CNPq under grants 304192/2019-8 and 140400/2021-4, the São Paulo Research Foundation (FAPESP) under grant 2013/07375-0 and the Coordenação de Aperfeiçoamento de Pessoal de Nível Superior - Brasil (CAPES) - Finance Code 001.

Authorship statement. The authors hereby confirm that they are the sole liable persons responsible for the authorship of this work, and that all material that has been herein included as part of the present paper is either the property (and authorship) of the authors, or has the permission of the owners to be included here.

References

[1] M. R. Correa, J. C. Rodriguez, A. M. Farias, D. de Siqueira, and P. R. B. Devloo. Hierarchical high order finite element spaces in $H(\mathrm{div}, \Omega) \times H^1(\Omega)$ for a stabilized mixed formulation of Darcy problem. *Comput. Math. with Appl.*, vol. 80, pp. 1117–1141, 2020.

[2] D. N. Arnold. Mixed finite element methods for elliptic problems. *Computer Methods in Applied Mechanics and Engineering*, vol. 82, n. 1, pp. 281 – 300, 1990.

[3] T. O. Quinelato, A. F. Loula, M. R. Correa, and T. Arbogast. Full H(div)-approximation of linear elasticity on quadrilateral meshes based on abf finite elements. *Computer Methods in Applied Mechanics and Engineering*, vol. 347, pp. 120 – 142, 2019.

[4] P. A. Raviart and J. M. Thomas. A mixed finite element method for second order elliptic problems. In W. Wunderlich, E. Stein, and K. J. Bathe, eds, *Math. Aspects of the F.E.M.*, number 606 in 1, pp. 292–315. Springer-Verlag, 1977a.

[5] T. Arbogast and M. R. Correa. Two families of H(div) mixed finite elements on quadrilaterals of minimal dimension. *SIAM J. Numer. Anal.*, vol. 54, n. 6, pp. 3332–3356, 2016.

[6] P. A. Raviart and J. M. Thomas. Primal hybrid finite element methods for 2nd order elliptic equations. *Math. Comp.*, vol. 31, n. 138, pp. 391–413, 1977b.

[7] D. N. Arnold, F. Brezzi, B. Cockburn, and D. Marini. Unified analysis of discontinuous Galerkin methods for elliptic problems. *SIAM J. Numer. Anal.*, vol. 39, n. 5, pp. 1749–1779, 2002.

[8] A. F. D. Loula, F. A. Rochinha, and M. A. Murad. Higher-order gradient post-processings for second-order elliptic problems. *Computer Methods in Applied Mechanics and Engineering*, vol. 128, pp. 361–381, 1995.

[9] M. R. Correa and A. F. D. Loula. Stabilized velocity post-processings for Darcy flow in heterogenous porous media. *Communications in Numerical Methods in Engineering*, vol. 23, pp. 461–489, 2007.

[10] A. F. D. Loula, M. R. Correa, J. N. C. Guerreiro, and E. M. Toledo. On finite element methods for heterogeneous elliptic equations. *International Journal of Solids and Structures*, vol. 45, pp. 6436–6450, 2008.